How to create giant Dzyaloshinskii–Moriya interactions? Analytical derivation and ab initio calculations on model dicopper(II) complexes

Mohammed-Amine Bouammali, Nicolas Suaud, Cyril Martins, Rémi Maurice, Nathalie Guihéry

The Journal of Chemical Physics

How to create giant Dzyaloshinskii Moriya Interactions? Analytical derivation and *ab initio* calculations on model dicopper(II) complexes

Authors: Mohammed-Amine Bouammali,[1] Nicolas Suaud,[1] Cyril Martins,[1] Rémi Maurice[2] and Nathalie Guihéry[1*]

Affiliations :
[1] Laboratoire de Chimie et Physique Quantiques, UMR5626, University of Toulouse 3, Paul Sabatier, 118 route de Narbonne, 31062 Toulouse, France
[2] SUBATECH, UMR CNRS 6457, IN2P3/IMT Atlantique/Université de Nantes, 4 rue A. Kastler, 44307 Nantes Cedex 3, France

*nathalie.guihery@irsamc.ups-tlse.fr

Abstract: This paper is a theoretical "proof of concept" on how the on-site first-order spin-orbit coupling can generate giant Dzyaloshinskii-Moriya interaction in binuclear transition metal complexes. This effective interaction plays a key role in strongly correlated materials, skyrmions, multiferroics, molecular magnets of promising use in quantum information science and computing. Despite this, its determination from both theory and experiment is still in its infancy and existing systems usually exhibit very tiny magnitudes. We derive analytical formulas that perfectly reproduce both the nature and the magnitude of the Dzyaloshinskii-Moriya interaction calculated using state-of-the-art *ab initio* calculations performed on model bicopper(II) complexes. We also study which geometrical structures/ligand-field forces would enable one to control the magnitude and the orientation of the Dzyaloshinskii Moriya vector in order to guide future synthesis of molecules or materials. This article provides an understanding of its microscopic origin and proposes recipes to increase its magnitude. We show that i) the on-site mixings of 3d orbitals rules the orientation and magnitude of this interaction, ii) increased values can be obtained by choosing more covalent complexes, iii) huge values (~1000 cm^{-1}) and controlled orientations could be reached by approaching structures exhibiting on-site first-order SOC, *i.e.* displaying an "unquenched orbital momentum".

I Introduction

Due to the fundamental contributions of Igor Dzyaloshinskii and Tôru Moriya in the magnetism field, the antisymmetric exchange is often referred to as the Dzyaloshinskii-Moriya interaction (DMI). The discovery of this interaction dates back to the middle of the twentieth century. It was invoked to rationalize the exotic behaviors of magnetization in materials, such as the weak ferromagnetism of hematite α-Fe_2O_3.[1] Based on phenomenological arguments, Dzyaloshinskii showed in 1958 that this interaction was due to the combination of low symmetry and relativistic effects, as it is the case for the Zero-Field Splitting (ZFS). Extending Anderson's theory of superexchange, Moriya then theorized this interaction.[2] He proposed a mechanism based on spin-orbit coupling (SOC) as being the microscopic origin of DMI and gave the orientation of the Dzyaloshinskii-Moriya (DM) vector according to crystal lattice symmetries. Another fundamental manifestation of DMI is the stabilization of magnetically modulated chiral structures with fixed rotation sense for the curling of the magnetization vector.[3] While long-period helical magnetic structures were experimentally identified by neutron diffraction in MnSi[4] and FeGe[5] in 1970's, in the 1980's theoretical investigations showed that these structures could be explained by DMI.[6,7] Since that period many modulated magnetic structures of this kind have been discovered in various classes of non-centro-symmetric magnetic crystals. In 1989 Bogdanov and Yablonskii predicted an important phenomenon: Dzyaloshinskii-Moriya interaction can stabilize one-dimensional spiral structures, but also two- and three-dimensional textures named skyrmions.[8,9] Since the experimental observation in 2010 of skyrmionic states in nanolayers of $Fe_{0.5}Co_{0.5}Si$ under magnetic field by Yu *et al*.[10] this discovery has opened new challenges in fundamental physics and technological applications in spintronics, data storage and quantum computing. One may also quote a particular effort in direction of spin-orbitronic devices in surface science where large DMI was observed using O_2 (paramagnetic) adsorbed on ferromagnetic surfaces.[11]

Among other manifestations, the DMI is also invoked in multiferroic materials.[12,13] For those materials that exhibit both polarization and magnetization, one of the major challenges is to maximize the magneto-electric coupling. Indeed**,** while high electric polarizations are observed in non-magnetic ferroelectric materials, very weak electric polarizations are obtained in ferromagnetic systems. Such a finding has led chemists to synthesize hybrid materials that have two (or more) layers of different materials, one being ferro- (or antiferro-) magnetic and the other one strongly ferroelectric.[14] These materials have two different populations of electrons, each of them being responsible for one of the properties. As a consequence, the control of polarization and magnetization requires the use of both electric and magnetic fields. The conception of non-hybrid materials, for which the same population of electrons would be responsible for both properties, would enable us to also control polarization through a magnetic field and magnetization using an electric field, provided that the magneto-electric coupling is large enough. In such systems, it has been established that polarization arising from the through-ligand spin current is proportional to the vector product between the centers A and B distance vector, $\mathbf{e}_{AB}$, and the DM $\mathbf{d}_{AB}$ vector. To maximize polarization in such systems therefore relies on the possibility to increase the DMI. Beyond the interest for multiferroic materials, maximizing magneto-electric coupling would be very useful in devices for quantum computing (for instance).[15–17] Indeed, the nanoscopic size of quantum bits makes them difficult to control by a magnetic field which is hardly focusable and a control by electric field is highly desirable.

The conditions of symmetry to have a non-zero DMI have been known for quite a long time, such as for instance allowing to have a non-zero antisymmetric component of the spin-spin coupling tensor in the context of the spin of the nucleus.[18] While only a few papers from theoretical chemists reporting calculations of the DMI have been published, many approaches have been used to compute symmetric anisotropy tensors.[19–23] The physical content of the local anisotropy tensor appearing in systems of

spin larger than ½ is quite well understood.[24–27] Concerning the anisotropy of the symmetric exchange tensor, analytical expressions of the axial D_{AB} and rhombic E_{AB} zero field splitting (ZFS) parameters have been derived for binuclear complexes (made of magnetic centers A and B) and *ab initio* calculations have been performed to precisely extract both parameters in the copper-acetate complex.[28] For a centrosymmetric system of two Ni(II) (spin S=1) the extraction of both the multispin spin[25] and the giant Hamiltonians[29] has already been performed and it was shown that a four-rank tensor was required to accurately reproduce the anisotropy of exchange. Reference[30] reports the study of model complexes of Ni(II) of various symmetries in which all parameters have been extracted. In this last work the magnitude of the DMI was very small and the theoretical effort was focused on the other parameters.

Works concerning the quantum chemical description of the DMI are rather scarse. One may quote for instance few papers by some of us focused on its dependence (both in magnitude and in orientation) to geometrical deformations,[31] and applications to materials,[32–34] and also a work by Atanasov et al..[35] Concerning the understanding of the electronic factors ruling the DMI, the literature is also quite incomplete. In his famous article, Moriya first derived this terms in an atomic orbital (AO) basis and with a crystal field picture in 1960. Decades later, this work was extended by Moskvin to include contributions from the bridging oxygens,[36] *i.e.* for not restricting the expression to the metal AOs. Note that in reference [26], computed wave functions were analyzed to propose first explanations concerning the specific deformations that were applied to the retained model complexes.

The present work aims at revisiting and completing these early and partial attempts to identify the electronic and geometric factors that rule the magnitude and the orientation of this vector and propose first analytical formulas that describe its components in a more general context (*i.e.* applicable to any binuclear complex of local spin S_i=1/2, independent from the local coordination environments and from the symmetry of the system). To determine these factors, we will focus our applications to simple model complexes constituted of two copper ions surrounded by chloride ligands. We should make clear here that this choice for model complexes is guided by two main reasons, (i) we are not aware of any available experimental data on actual dicopper(II) complexes and (ii) cases for which experimental data is available present much too complex situations for a first *ab initio* mechanistic study. One may quote for instance a diferric complex[37] (correlation is tricky on iron complexes) or a tricopper(II) one[38] (the occurrence of three active centers poses more questions such as the correct application of the permutation relationship and will be the subject of a forthcoming work). Consequently, it is wise to start establishing accurate quantum chemical methodologies and general and tractable analytical formulas by focusing on model dicopper(II) complexes.

The article is organized as follows. In section II, analytical expressions of the DM vector components are derived and the surface of its components as a function of the different mixings between d orbitals in the singlet and the triplet states is provided. Section III contains the computational information and section IV presents the results obtained on two different model complexes in which specific deformations are applied to create DMI.

II. Analytical expressions of the DM components

The DM vector appears in anisotropic Hamiltonian for the description of magnetic systems presenting magnetic anisotropy. For a binuclear compound constituted of two spins S_i=1/2, the multispin Hamiltonian writes:

$$\hat{H}^{model} = J_{AB}\vec{\hat{S}}_A.\vec{\hat{S}}_B + \vec{\hat{S}}_A.\bar{\bar{D}}_{AB}.\vec{\hat{S}}_B + \vec{d}_{AB}.\vec{\hat{S}}_A \times \vec{\hat{S}}_B \quad (1)$$

where $\vec{\hat{S}}_I$ is the spin operator on center I={A,B}, J_{AB} is the isotropic magnetic coupling, $\overline{\overline{D}}_{AB}$ is the symmetric magnetic anisotropy tensors of exchange and $\vec{d}_{AB}$ is the antisymmetric anisotropy tensor *i.e.* the DM vector. Subtracting the isotropic contribution to the exchange anisotropic tensor, one has access to the axial D_{AB} and rhombic E_{AB} parameters while the three components of DM vector are called d_x, d_y and d_z, in practice dependent on the axis frame used in the calculations. Let us call *a* and *b* the local magnetic orbitals of the triplet state; *i.e.* the orbitals bearing the unpaired electrons. The magnetic orbitals have tails on the ligands and result from local mixings between d orbitals. Both the mixings and the tails are different in the triplet and singlet states that are formed by the electronic coupling of the two unpaired electrons. We will call *a'* and *b'* the singlet magnetic orbitals. One should note that usually in model spin Hamiltonian the spatial part is assumed to be common to all states described by the model and only the spin degrees of freedom are considered. As will be shown in this section, the DMI is strictly zero for identical singlet and triplet orbitals. It is however possible to account for the difference between the two sets of orbitals by introducing flexibility in the coefficients of the determinants on which the two wave functions are expressed. The spin-orbit interaction couples the M_S components of the two electronic states differently generating the components of both symmetric and antisymmetric anisotropic tensors. The model Hamiltonian matrix in the coupled basis, for which S_0, T_0 and $T_{\pm1}$ stand for the singlet and triplet M_S=0 and M_S=±1 spin components, *i.e.* in the $\{T_1 = |ab\rangle \;;\; T_0 = \left|\frac{a\bar{b}-b\bar{a}}{\sqrt{2}}\right\rangle \;;\; T_{-1} = |\overline{ab}\rangle \;\;;\;\; S_0 = \left|\frac{a'\overline{b'}+b'\overline{a'}}{\sqrt{2}}\right\rangle\}$ basis, writes:

$$\left(\hat{H}^{model}\right) = \begin{array}{c} \\ \langle ab| \\ \left\langle\frac{a\bar{b}-b\bar{a}}{\sqrt{2}}\right| \\ \langle\overline{ab}| \\ \left\langle\frac{a'\overline{b'}+b'\overline{a'}}{\sqrt{2}}\right| \end{array} \begin{array}{c} \begin{array}{cccc} T_1 = |ab\rangle & T_0 = \left|\frac{a\bar{b}-b\bar{a}}{\sqrt{2}}\right\rangle & T_{-1} = |\overline{ab}\rangle & S_0 = \left|\frac{a'\overline{b'}+b'\overline{a'}}{\sqrt{2}}\right\rangle \end{array} \\ \begin{pmatrix} \frac{J}{4}+\frac{D_{zz}}{4} & \frac{D_{xz}-iD_{yz}}{2\sqrt{2}} & \frac{(D_{xx}-D_{yy}-2iD_{xy})}{4} & \boldsymbol{\frac{d_y+id_x}{2\sqrt{2}}} \\ \frac{D_{xz}+iD_{yz}}{2\sqrt{2}} & \frac{J}{4}-\frac{D_{zz}}{4}+\frac{(D_{xx}+D_{yy})}{4} & -\frac{D_{xz}-iD_{yz}}{2\sqrt{2}} & \boldsymbol{-\frac{id_z}{2}} \\ \frac{(D_{xx}-D_{yy}+2iD_{xy})}{4} & -\frac{D_{xz}+iD_{yz}}{2\sqrt{2}} & \frac{J}{4}+\frac{D_{zz}}{4} & \frac{d_y-id_x}{2\sqrt{2}} \\ \boldsymbol{\frac{d_y-id_x}{2\sqrt{2}}} & \boldsymbol{\frac{id_z}{2}} & \boldsymbol{\frac{d_y+id_x}{2\sqrt{2}}} & -\frac{3J}{4}-\frac{D_{zz}}{4}-\frac{(D_{xx}+D_{yy})}{4} \end{pmatrix} \end{array} \quad (2)$$

where, D_{xx}, D_{xy}, ... are the components of the $\overline{\overline{D}}_{AB}$ symmetric exchange tensor. The DMI only couples the singlet with the three M_S components of the triplet. Its determination therefore only requires to calculate the SOC matrix elements between these two electronic states.

The off diagonal elements of the SOC matrix can be analytically calculated using the spin-orbit operator $\hat{H}^{SO} = \xi\left(\vec{\hat{l}}_1.\vec{\hat{s}}_1 + \vec{\hat{l}}_2.\vec{\hat{s}}_2\right)$ where $\vec{\hat{l}}_\iota$ and $\vec{\hat{s}}_\iota$ are the angular and spin momenta respectively of electron *i* and ξ is the spin-orbit constant (we consider a spherical approximation of the SOC and identical magnitudes on both sites). The action of the spin operator gives:

$$\left\langle\frac{|a\overline{b'}|+|b'\overline{a'}|}{\sqrt{2}}\right|\xi\left(\vec{\hat{l}}_1.\vec{\hat{s}}_1+\vec{\hat{l}}_2.\vec{\hat{s}}_2\right)\left||ab|\right\rangle = \frac{1}{2\sqrt{2}}(\langle b'|\xi l^+|b\rangle\langle a'|a\rangle - \langle a'|\xi l^+|a\rangle\langle b'|b\rangle) \quad (3)$$

$$\left\langle\frac{|a\overline{b'}|+|b'\overline{a'}|}{\sqrt{2}}\right|\xi\left(\vec{\hat{l}}_1.\vec{\hat{s}}_1+\vec{\hat{l}}_2.\vec{\hat{s}}_2\right)\left|\overline{|ab|}\right\rangle = \frac{1}{2\sqrt{2}}(\langle a'|\xi l^-|a\rangle\langle b'|b\rangle - \langle b'|\xi l^-|b\rangle\langle a'|a\rangle) \quad (4)$$

$$\left\langle\frac{|a\overline{b'}|+|b'\overline{a'}|}{\sqrt{2}}\right|\xi\left(\vec{\hat{l}}_1.\vec{\hat{s}}_1+\vec{\hat{l}}_2.\vec{\hat{s}}_2\right)\left|\frac{|a\bar{b}|-|b\bar{a}|}{\sqrt{2}}\right\rangle = \frac{1}{2}(\langle a'|\xi l^z|a\rangle\langle b'|b\rangle - \langle b'|\xi l^z|b\rangle\langle a'|a\rangle) \quad (5)$$

These equations show that if for symmetry reason a=b (thus a'=b') the DMI is strictly zero. In the case of two symmetrically equivalent magnetic centers it is therefore necessary to locally mix differently the atomic orbitals (hybridization) on centers A and B in order to create DMI. In order to maximize this interaction, the most interesting cases are such that i) a symmetry lowering leads to specific local orbital mixings that ultimately lead to a significant DMI, ii) the difference of the MO coefficients between the singlet and triplet states is sizeable and iii) the effect of the angular momentum is important, *i.e.* the magnetic orbitals have large $|M_l|$ components of the angular momentum. In the case of transition metal centers, the most efficient mixing would involve the spherical harmonics d_{2+} and d_{2-}, *i.e.* the d_{xy} and d_{x2-y2} real orbitals. One may note that with lanthanides the $f_{\pm 3}$ spherical harmonics would be a priori the most interesting ones to be involved in the mixing. Nevertheless, the singlet and triplet orbitals would be very similar due to the weak interactions of the very concentrate 4f orbitals with the ligand ones, which should finally result in a weak if not negligible DMI. Finally, as we will see in the section devoted to applications, the difference between the singlet and triplet molecular orbitals (MOs) plays a crucial role. As covalence introduces ionic components in the singlet wave function, it induces a different relaxation of the singlet MOs, which should increase the DM vector components.

In order to show the physical content of the d_x, d_y and d_z components, we have considered the mixing of all d orbitals two by two that could be obtained from distortions of the coordination sphere. Starting from delocalized MOs obtained from combinations of the overlapping d orbitals, it is always possible to define local orthogonal new d orbitals called d_1^A and d_2^A on center A and d_1^B and d_2^B on center B. The local orbitals *a* and *b* can be expressed as:

$$\begin{aligned} a &= \alpha d_1^A + \beta d_2^A \\ b &= -\alpha d_1^B + \beta d_2^B \\ a' &= \alpha' d_1^A + \beta' d_2^A \\ b' &= -\alpha' d_1^B + \beta' d_2^B \end{aligned} \qquad (6)$$

Such mixings correspond to symmetric distortions either along X, Y or Z axis, the SOC is always proportional to:

$$\Delta = \xi[\alpha\beta(\alpha'^2 - \beta'^2) - \alpha'\beta'(\alpha^2 - \beta^2)] \qquad (7)$$

Figure 1 represents Δ/ξ as a function of the parameters α and α'. β and β' are always positive and are fixed by the orbitals normalization, *i.e.* $\alpha^2+\beta^2=1$ and $\alpha'^2+\beta'^2=1$. In a first place, one should note that as the singlet and triplet orbitals are usually quite similar in magnetic complexes, real situations are close to the straight line α=α' (in black and bold on the figure on the right). Nevertheless, the variation of $|\Delta|$ is very abrupt close to this line and reaches the maximum of $|0.5\xi|$ for $(\alpha^2 - \alpha^4) \pm (\alpha'^2 - \alpha'^4) = 1/4$ and is zero for the circle $\alpha^2 + \alpha'^2 = 1$ when α and α' are of opposite sign, *i.e.* for non-physical values of the coefficients. Indeed, in magnetic systems the magnetic orbitals are very similar in all magnetic states of the same configuration and this is what underlies the validity of spin Hamiltonians for which the spatial part of all wave functions is factorized.

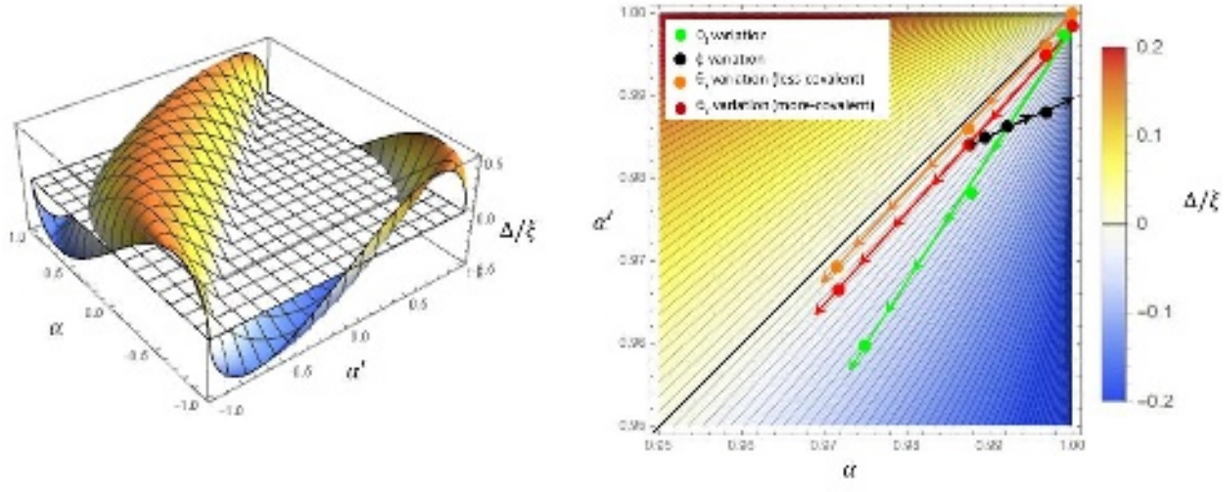

Figure 1: Δ/ξ surface as a function of the parameters α and α' (left) and a portion in the physical region of its contour plot (right). The calculated values obtained for the different studied complexes (see the Application section) are also reported (right). Arrows indicate direction towards larger deformations.

The different components of the DM vector can be deduced from the expressions reported in Table 1. Of course combining the various contributions, these results can be used to describe mixings of three or more local orbitals. As expected, the biggest DM components are obtained from the application of the $\hat{l}_z\hat{s}_z$ operator (which generates the d_z components) and for the largest (in absolute value) angular momentum Z component quantum numbers M_l =±2.

d_1	d_2	Matrix elements of the SOC
$d_{x^2-y^2}$	d_{xy}	$\langle S_0\lvert\hat{H}^{SO}\rvert T_0\rangle = \frac{id_z}{2} = -2i\Delta$
$d_{x^2-y^2}$	d_{xz}	$\langle S_0\lvert\hat{H}^{SO}\rvert T_{\pm1}\rangle = \frac{d_y}{2\sqrt{2}} = -\frac{\Delta}{\sqrt{2}}$
$d_{x^2-y^2}$	d_{yz}	$\langle S_0\lvert\hat{H}^{SO}\rvert T_{\pm1}\rangle = \mp\frac{id_x}{2\sqrt{2}} = \mp\frac{i\Delta}{\sqrt{2}}$
d_{xy}	d_{xz}	$\langle S_0\lvert\hat{H}^{SO}\rvert T_{\pm1}\rangle = \mp\frac{id_x}{2\sqrt{2}} = \pm\frac{i\Delta}{\sqrt{2}}$
d_{xy}	d_{yz}	$\langle S_0\lvert\hat{H}^{SO}\rvert T_{\pm1}\rangle = \frac{d_y}{2\sqrt{2}} = -\frac{\Delta}{\sqrt{2}}$
d_{xz}	d_{yz}	$\langle S_0\lvert\hat{H}^{SO}\rvert T_0\rangle = \frac{id_z}{2} = -i\Delta$

d_{xz}	d_{z^2}	$\langle S_0 \lvert \hat{H}^{SO} \rvert T_{\pm 1} \rangle = \frac{d_y}{2\sqrt{2}} = -\frac{\Delta\sqrt{3}}{\sqrt{2}}$
d_{yz}	d_{z^2}	$\langle S_0 \lvert \hat{H}^{SO} \rvert T_{\pm 1} \rangle = \mp\frac{id_x}{2\sqrt{2}} = \pm\frac{i\Delta\sqrt{3}}{\sqrt{2}}$

Table 1: Non-zero elements of the SOC matrix involving the DM vector d_x, d_y and d_z components resulting from the couplings between the various states obtained by mixings of d_1 and d_2 orbitals (see equations 5, 6 and 7). An interchange between d_1 and d_2 leads to a change between α (α') and β (β') in Δ.

III. Computational information

Ab initio calculations have been performed using the MOLCAS8.0 code.[39–41] In order to get zeroth order correlated wave functions and to optimize average orbitals for several states, the Complete Active Space Self Consistent Field (CASSCF) method has been employed.[42] CAS(6,4) calculations (6 active electrons/4 active MO) on 4 triplet and 4 singlet states have been performed for the model complexes **1** and **2** ($Cu_2Cl_7^{3-}$ and $Cu_2Cl_5^{-}$, respectively, see Figures 2 and 4 for more details) while CAS(18,10) calculations on 25 triplet and 25 singlet states have been done for complex **1'** (also $Cu_2Cl_7^{3-}$, but with different applied deformations than for **1**, as can be seen from the comparison of Figures 2 and 3). As the studied systems are model complexes, dynamic correlation that would be brought by post-CASSCF calculations has been neglected even if its effect on the wave function of the electronic states is non-negligible. Accurate calculations of the wave function coefficients require a sophisticated method such as Casdiloc that works with orthogonal local orbitals to restrict the Configuration Interaction space using locality criteria.[43,44] Nevertheless, it is much less important on the SO spectrum of the lowest states. Its account would not change the qualitative results and would not affect in any way the more general scope of this article, which essentially consists in establishing reliable analytical formulas. The Spin-Orbit State-Interaction (SO-SI) method[45] implemented in MOLCAS has been used in a second step in order to account for the SOC between the various states. The quality of the results of the latter method for the calculation of SO states of transition metal complexes is well established for the determination of anisotropy in transition metal complexes.[26]

In order to extract the DM vector components, two procedures have been used: i) direct calculation from the off-diagonal elements of the SO-SI matrix (see equation 2), ii) calculation from the electronic wave function coefficients and the here proposed formulas. Note that if post-CASSCF energies were used while maintaining the CASSCF wave functions for computing the off-diagonal SOC matrix elements (this is a spread approach), the same values would naturally be obtained as these elements only depend on the wave functions, which further supports the choice for using only the CASSCF energies and wave functions in the present context.

The confrontation of our equations to *ab initio* results requires to determine the coefficients α, β, α' and β'. Since the atomic orbitals overlap, they do not form an orthonormal basis set as those of equation 6. Besides, the optimized MOs are orthonormal but have tails onto the ligands and are therefore no more purely atomic. An alternative way consists in using the coefficients of the determinants after relocalizing the orbitals on the left and right magnetic centers. The Projected Atomic Orbitals Cholesky method of localization was used.[46] In the case of a mixing between two d

orbitals on each center, the analytical expression of the four electronic states spin components as functions of the local orbitals reads:

$$
\begin{aligned}
{}^3\Psi_{ms=1} &= -\alpha^2(d_1^A d_1^B) + \beta^2(d_2^A d_2^B) + \alpha\beta(d_1^A d_2^B - d_2^A d_1^B) \\
{}^3\Psi_{ms=-1} &= -\alpha^2\left(\bar{d}_1^A \bar{d}_1^B\right) + \beta^2\left(\bar{d}_2^A \bar{d}_2^B\right) + \alpha\beta(\bar{d}_1^A \bar{d}_2^B - \bar{d}_2^A \bar{d}_1^B) \\
{}^3\Psi_{ms=0} &= \frac{1}{\sqrt{2}}[-\alpha^2\left(d_1^A \bar{d}_1^B - d_1^B \bar{d}_1^A\right) + \beta^2\left(d_2^A \bar{d}_2^B - d_2^B \bar{d}_2^A\right) + \alpha\beta(d_1^A \bar{d}_2^B + d_1^B \bar{d}_2^A - d_2^B \bar{d}_1^A - d_2^A \bar{d}_1^B)] \\
{}^1\Psi_{ms=0} &= \frac{1}{\sqrt{2}}[-\alpha'^2\left(d_1^A \bar{d}_1^B + d_1^B \bar{d}_1^A\right) + \beta'^2\left(d_2^A \bar{d}_2^B + d_2^B \bar{d}_2^A\right) + \alpha'\beta'(d_1^A \bar{d}_2^B - d_1^B \bar{d}_2^A + d_2^B \bar{d}_1^A - d_2^A \bar{d}_1^B)]
\end{aligned}
\tag{8}
$$

Ab initio wave-function therefore gives access to the four interesting parameters. One should note that two values can be calculated using the analytical formulas given in Table 1: i) in the first one the $\alpha\beta^{Calc}$ ($\alpha'\beta'^{Calc}$) product is taken as being $\sqrt{\alpha'^2\beta'^2}$ ($\sqrt{\alpha'^2\beta'^2}$) while ii) in the second one it is directly the coefficients of the corresponding determinants in the *ab initio* wave function (see equation 8). Of course the second extraction provides more precise values as CASSCF wave functions of the lowest states can mix with those of excited states, inducing a change of the relative coefficients of the various determinants of equation 8.

IV Applications

A. How to generate a single d_y component of the DMI?

In the article[31] we have shown that an efficient way to generate a single component DMI with a definite orientation was to impose a bending angle between two planar moieties, each of them involving a transition metal ion. The model complex **1** $Cu_2Cl_7^{3-}$ (see Figure 2 left) has been chosen to illustrate both the link between the orbital mixing and the nature of the DMI, and the quantitative validity of the here proposed formula (see Table 1). This section also aims at showing the importance of the difference between the singlet and triplet orbitals and how covalence affects this difference and may therefore be a significant ingredient to control DMI (by an appropriate choice of ligands).

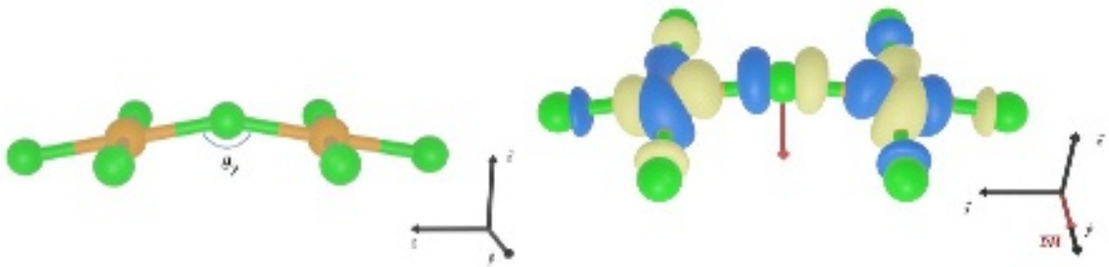

Figure 2 : Model complex **1** (left) and angular deformation θ_y generating a d_y component of the DMI; One magnetic MO (right) of the triplet state resulting from the mixing between the $d_{x^2-y^2}$ and d_{xz} orbitals for the angle θ_y=160°. The calculated DM vector (in red) is also represented (right) centered on the origin of the axes frame (middle of the fragment Cu(II)-Cu(II)).

The triplet MOs (Figure 2 right) result from a mixing between the $d_{x^2-y^2}$ and d_{xz} orbitals as expected from the applied bending. From Table 1, such a mixing induces a DMI in the Y direction, as can be seen in the computed vector represented in Figure 2. Table 2 shows the values of the DMI extracted from either the off-diagonal element coupling the singlet and the triplet in the SO-RASSI matrix or using the here proposed formula. For comparison we have used either the *ab initio* coefficients

$\alpha\beta^{abinitio}$ or the $\alpha\beta^{Calc} = \sqrt{\alpha'^2\beta'^2}$. The results confirm that more precise values are obtained when using the *ab initio* coefficients. It is worth noting that even if these changes are relatively small, the sensitivity of the DMI to the coefficients is quite important and one must use the *ab initio* ones preferably. From these results we can draw some qualitative conclusions:

- The proposed formula especially when using *ab initio* coefficients furnishes very accurate values of the DMI. The slight differences between the off-diagonal matrix elements and the DMI calculated from the analytical formula comes from the fact that we are using a unique spin-orbit constant that has been fixed to that of the Cu^{2+} ion, *i.e.* ξ =830 cm^{-1}.[47] Note that usually, using the free-ion value for complexes may lead to an overestimation of the SOC (it is commonly admitted that covalence leads to a reduction of the SOC constant).
- The DMI which is strictly zero at 180° for symmetry reasons (centro-symmetric molecule) increases with the bending as expected. The calculated DMI values as functions of the deformation angle are reported in Figure 1 (right, orange dots). We observe that the values increase with the deformation, *i.e.* dots move away from the diagonal line for which $d_y = 0$.
- Last but not least the DMI is much larger for the complex that has shorter bonds between the chlorides and the Cu(II) ions, *i.e.* for the most covalent complex. Comparing the coefficients of the triplet and the singlet, one may note that the mixing between the local orbitals is higher in the singlet and that it increases with covalence, resulting in more different orbitals between the two states. The red dots that are reported in Figure 1 (right) are shifted down in comparison to the less covalent complex DMI (orange dots) which shows that the singlet coefficients are more affected (*i.e.* the α' change).

Distances Cu^{2+}-Cl^-	θ	α^2	β^2	$\alpha\beta$ calculated	$\alpha\beta$ *ab initio*	α'^2	β'^2	$\alpha'\beta'$ calculated	$\alpha'\beta'$ *ab initio*	$\lvert d_y \rvert$ from SO-SI	$\lvert d_y \rvert$ from formulas * α.β and α'.β ' *ab initio* / calculated
2.0 Å	150°	.9442	.0494	.2161	.2217	.9340	.0616	.2398	.2357	28	29 /43
	160°	.9753	.0223	.1475	.1512	.9682	.0294	.1688	.1648	22	25/ 37
	170°	.9937	.0060	.0774	.0764	.9896	.0080	.0890	.0848	12	15 / 20
	180°	1.000	.0000	.0000	.0000	.9969	.0000	.0000	.0000	0	0 / 0
2.2 Å	150°	.9438	.0507	.2188	.2216	.9394	.0564	.2301	.2284	13	14 / 20
	160°	.9750	.0229	.1495	.1513	.9722	.0263	.1599	.1578	10	12 / 18
	170°	.9935	.0060	.0772	.0765	.9922	.0070	.0833	.0806	6	7 / 10
	180°	1.000	.0000	.0000	.0000	1.0000	.0000	.0000	.0000	0	0 /0

Table 2: values in cm^{-1} of the DMI extracted from either the off-diagonal matrix element of the SO-RASSI method or the here proposed formula (see text) for complex **1** with two different Cu(II)-Cl^- (bridging) distances. The coefficients of the determinants are either calculated from $\sqrt{\alpha^2\beta^2}$ (see computational information) or extracted from the *ab initio* wave functions. * see Table 1.

B. DMI with two components

The model complex **1'** $Cu_2Cl_7^{3-}$ in which we have added a second deformation to the previous one is represented in Figure 3 left. The distortions of complex **1'** are such that in addition to the θ_y =170°

bending angle we have introduced a θ_z= 160° angle between the two moieties in the XOY plane around the Cl^- bridging ligand. The final angle (Cu-Cl-Cu) is 151.8°. Such a deformation generates a mixing of all d orbitals so that:

$$\begin{aligned} a &= \alpha d_{x^2-y^2} + \beta d_{xy} + \gamma d_{xz} + \delta d_{yz} + \varepsilon d_{z^2} \\ b &= \alpha d_{x^2-y^2} - \beta d_{xy} - \gamma d_{xz} + \delta d_{yz} + \varepsilon d_{z^2} \\ a' &= \alpha' d_{x^2-y^2} + \beta' d_{xy} + \gamma' d_{xz} + \delta' d_{yz} + \varepsilon' d_{z^2} \\ b' &= \alpha'^{d_{x^2-y^2}} - \beta'^{d_{xy}} - \gamma'^{d_{xz}} + \delta'^{d_{yz}} + \varepsilon'^{d_{z^2}} \end{aligned} \qquad (9)$$

This mixing can be observed in the drawing of one magnetic orbital of the triplet state (Figure 3 right). The DM vector lies in the (YZ) plane (*i.e.* it has two components d_y and d_z) and has a larger component in the Z direction than in the Y one.

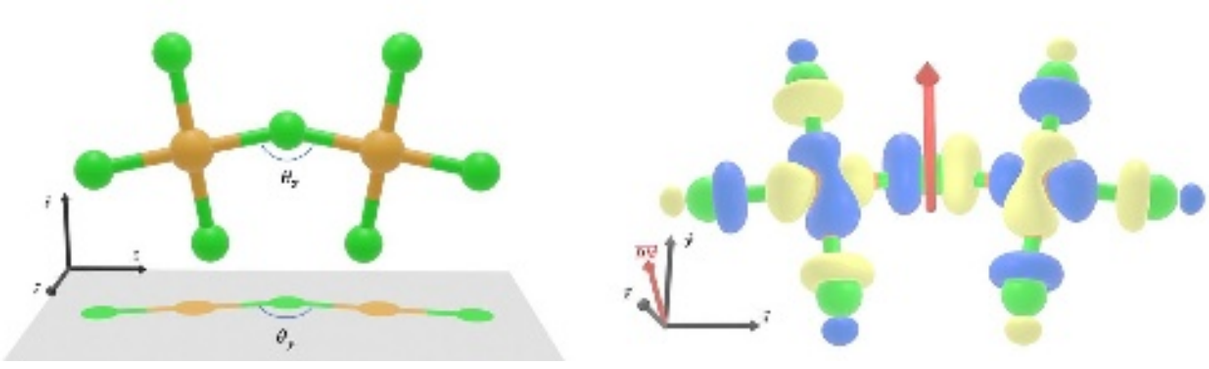

Figure 3 : Model complex **1'** (left) with angular deformations θ_y and θ_z respectively generating d_y and d_z components of the DMI; One magnetic MO (right) resulting from the mixing between all d orbitals for the angles θ_y =170° and θ_z= 160°. The calculated DM vector (in red) is also represented (right) centered on the origin of the axes frame (middle of the fragment Cu(II)-Cu(II)).

From Table 1 and equation 9 (and taking care of the sign of the coefficients in these orbitals), one sees that only d_y and d_z components are generated. d_z comes from mixings between i) $d_{x^2-y^2}$ and d_{xy} and ii) d_{xz} and d_{yz}. d_y is produced by the mixings between i) $d_{x^2-y^2}$ and d_{xz} , ii) d_{z^2} and d_{xz}, iii) d_{yz} and d_{xy}. In the studied geometry the coefficients on the d_{yz} and d_{z^2} orbitals are so small that the weights of the determinants involving these orbitals are less than 1%. It is therefore possible to limit our expressions of the DMI components to the main contributions:

$$\begin{aligned} d_z &= -4\xi(\alpha'\beta'(\alpha^2-\beta^2) - \alpha\beta(\alpha'^2-\beta'^2)) \\ d_y &= -\xi\sqrt{6}(\alpha'\gamma'(\alpha^2-\gamma^2) - \alpha\gamma(\alpha'^2-\gamma'^2)) \end{aligned} \qquad (10)$$

Table 3 reports the values of the DMI components extracted from the SO-RASSI matrix and calculated using equations 10, together with the coefficients of the *ab initio* wave functions. Here again we can conclude that the values are in perfect agreement with those predicted from our analytical formula. The results show that as expected the best way to generate an important value of DMI component in to induce a SOC between the singlet and the triplet through the $\hat{l}_z\hat{s}_z$ operator (see Table 1) resulting from a mixing between the $d_{x^2-y^2}$ and d_{xy} orbitals. This induces a d_z component which is much larger than the d_y one (almost twice the value in our complex **1'**). Note that in the general case, we should not exclude the possibility of a significant contribution coming from the $\hat{l}_z\hat{s}_z$

operator associated with the mixing of the d_{xz} and d_{yz} orbitals. Nevertheless, the expected effect would be lower due to the respective $|M_L|$ values (1 in d_{xz} and d_{yz} orbitals *vs.* 2 in $d_{x^2-y^2}$ and d_{xy} ones). In other words, equation (9) is general and one must not neglect any term a priori without analyzing the content of the wave functions obtained in the considered complex.

α^2	β^2	$\alpha\beta$	α'^2	β'^2	$\alpha'\beta'$	$\lvert d_z \rvert$ from SO-SI	$\lvert d_z \rvert$ from formulas *
.8765	.0971	.2926	.8644	.1041	.2991	36	36
α^2	γ^2	$\alpha\beta$	α'^2	γ'^2	$\alpha'\beta'$	$\lvert d_y \rvert$ from SO-SI	$\lvert d_y \rvert$ from formulas *
.8765	.0210	.1386	.8644	.0264	.1477	19	17

Table 3: values in cm^{-1} of the DMI components extracted from either the off-diagonal matrix element of the SO-RASSI method or the here proposed formulas (see text) for complex **1'**. The coefficients of the determinants are extracted from the *ab initio* wave functions. * see Table 1.

C. First-order SOC: a recipe to generate huge DMI

As seen in the previous subsection, large values of DMI can be obtained from the mixing between the $d_{x^2-y^2}$ and d_{xy} orbitals. In the paper[48] some of the authors have shown that approaching first-order SOC makes it possible to multiply the value of the axial parameter *D* of ZFS tenfold (or more). We followed the same approach in the next application. In order to generate a quasi-degeneracy between the $d_{x^2-y^2}$ and d_{xy} orbitals, we have imposed a local C_3 symmetry axis. For this purpose, the model complex **2** $Cu_2Cl_5^-$ now has a coordination of 3 around each Cu(II) ion. We have then varied the bending angle between the bridging chloride and the two Cu(II) ions, that controls the mixing between the two orbitals. Of course, as the anisotropic spin Hamiltonian becomes irrelevant in the case of a first order SOC, we have also changed the ϕ angle between the external ligands in order to gradually move away from the degeneracy. Note that as the deformations are carried out only within the (XOY) plane, they induce the mixing of only $d_{x^2-y^2}$ and d_{xy} orbitals. Complex **2** is pictured in Figure 4 (left) as well as the deformation angles θ_z and ϕ. On Figure 4 (right) one may appreciate the expected mixing between the orbitals and the direction strictly along Z of the DM vector.

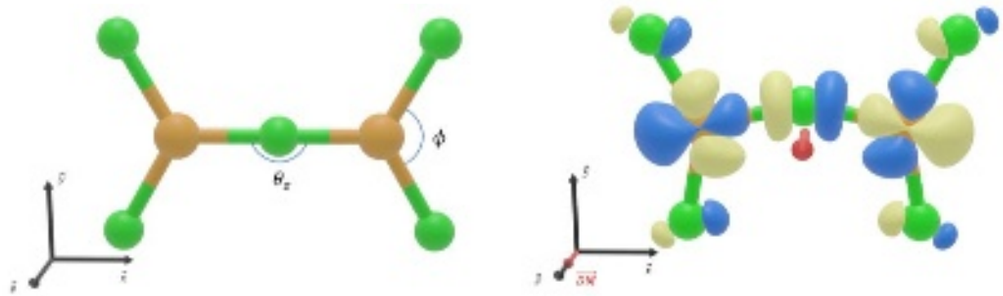

Figure 4: Model complex **2** $Cu_2Cl_5^-$ (left) with angular deformations θ_z and ϕ generating a d_z component of the DMI; One magnetic MO (right) of the triplet state resulting from the mixing between $d_{x^2-y^2}$ and d_{xy} orbitals for the angles θ_z=160° and ϕ=140°. The calculated DM vector (in red) is also represented (right) centered on the origin of the axes frame (middle of the segment Cu(II) – Cu(II)).

Table 4 presents the results obtained for ϕ=140° and various θ_z angles. The evolution of the DM vector follows the predicted behavior (see green dots on Figure 1), *i.e.* for small deformations of θ_z from 180° the DMI increases sharply and then attenuates even before reaching an equal mixing of the $d_{x^2-y^2}$ and d_{xy} orbitals. One may note that quite large values are obtained as this mixing is the most efficient to create large DMI.

θ_z	α^2	β^2	$\alpha\beta$	α'^2	β'^2	$\alpha'\beta'$	$\lvert d_z \rvert$ from SO-SI	$\lvert d_z \rvert$ from formulas *
140°	.7464	.2380	.4394	.6986	.3118	.4533	198	200
145°	.8131	.1731	.3929	.7670	.2418	.4184	204	204
150°	.8689	.1194	.3395	.8266	.1802	.3745	205	203
155°	.9147	.0762	.2806	.8757	.1291	.3268	199	214
160°	.9504	.0432	.2177	.9210	.0816	.2664	181	196
165°	.9757	.0207	.1540	.9569	.0438	.1990	152	164
170°	.9842	.0148	.1207	.9726	.0264	.1604	110	118
175°	.9981	.0028	.0433	.9945	.0035	.0622	58	63

Table 4: values in cm^{-1} of the DMI extracted from either the off-diagonal matrix element of the SO-RASSI method or the here proposed formula (see text) for complex **2** for ϕ=140° and various θ_z angles. The coefficients of the determinants are extracted from the *ab initio* wave functions. * see Table 1.

Table 5 explores the impact of the deformations which make it possible to approach the first-order SOC regime, *i.e.* for a fixed θ_z = 170° and various values of ϕ. Close to 120° one reaches huge values of the DMI. This deformation is the most efficient one to create giant DMI, as can be seen in Figure 1 (black dots). One may note that the coefficients of the triplets are now those that are the most affected by the deformation (α changes). Looking at the coefficients reported in Table 4, one sees that approaching ϕ=120° the nature of the wave functions changes due to strong mixings with excited states. In this "close to" first-order SOC regime, the spectrum becomes almost degenerate (see Figure 5). As a consequence, the anisotropic spin Hamiltonian that can only reproduce the first singlet and triplet states becomes irrelevant. The modeling that we propose here is no longer adapted to a precise extraction of the DMI. Indeed, its physical origin now comes as much from the important SOC between the different states as from their strong electronic mixing.

ϕ	α^2	β^2	$\alpha\beta$ *ab init*	α'^2	β'^2	$\alpha'\beta'$ *ab init*	$\lvert d_z \rvert$ from SO-SI	$\lvert d_z \rvert$ from formulas *
120°	.6531	.0647	.2056	.9904	.1311	.3603	1406	1522
130°	.9938	.0008	.0290	.9761	.0242	.1537	226	243
140°	.9842	.0148	.1207	.9726	.0264	.1604	110	118
160°	.9789	.0210	.1433	.9701	.0276	.1636	65	69

180°	.9775	.0225	.1483	.9683	.0275	.1630	53	56

Table 5: values in cm^{-1} of the DMI extracted from either the off-diagonal matrix element of the SO-RASSI method or the here proposed formula (see text) for complex **2** for θ_z=170° and various ϕ angles. The coefficients of the determinants are extracted from the *ab initio* wave functions. * see Table 1.

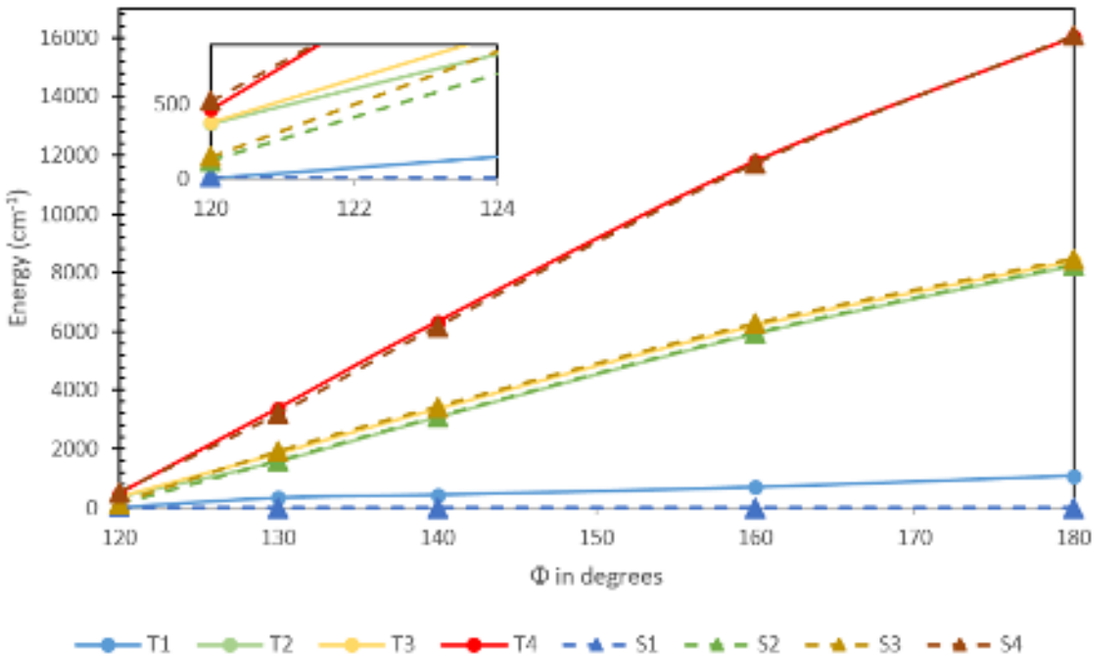

Figure 5: Spectrum in cm^{-1} of the lowest states obtained for θ=170° as a function of ϕ. Singlet Si and triplet Ti states are numbered following their energetic order from lowest to highest.

IV Conclusion:

In this paper we have derived analytical formulas that relate the DM vector components with the coefficients of the electronic wave functions of the lowest singlet and triplet states resulting from the coupling between two unpaired electrons located on two magnetic ions. In order to validate these formulas different model complexes have been studied. We have imposed various geometrical distortions that enabled us to study the nature and magnitude of the DM vector components. Naturally, we have chosen to express the MOs in specific axis frames with respect to the molecular symmetry elements, for the sake of simplicity. Nevertheless, we stress that our approach can be attempted in any arbitrary axis frame without altering the result, *i.e.* the orientation and magnitude of the DMI. The main conclusions are the following:

- First, the formulas provide quantitative agreement with the *ab initio* results except when we are close to first-order SOC.
- It allows to rationalize both the orientation and the magnitude of the DM vector as functions of the mixings between the d orbitals of the metal ions. This is an alternative to the reasoning of Moriya, which was based on AOs. We believe that orbital mixings are currently more intuitive to theoretical and experimental chemists than excitations between pure AOs, and thus that this new language will later prove to be useful in the molecular magnetism field. Indeed, since the orbital mixings are directly

linked to the ligand field, this new understanding will pave the way to synthetic chemistry for the design of complexes with controlled DMI.

- The most efficient way to produce large DMI is to mix the $d_{x^2-y^2}$ and d_{xy} orbitals in the magnetic orbitals which generates the d_z component of the DM vector. To further enlarge its magnitude one may also increase covalence between the magnetic centers since the difference between the singlet and triplet orbitals plays a major role on it. Note that it is also possible in principle to play on the mixture between the d_{xz} and d_{yz} orbitals, even if the resulting DMI is expected to be of lesser amplitude.
- Finally, to reach giant DMI, the recipe is to generate first-order SOC, in particular in near orbitally-degenerate situations (ideally between the $d_{x^2-y^2}$ and d_{xy} orbitals). Indeed, it is desirable to approach the degeneracy regime but without fully reaching it. Otherwise, as the spectrum becomes degenerate, the spin Hamiltonian approach becomes irrelevant and the here proposed modelling is no longer appropriate. In such a case, both a new model describing all the degenerate states and a method of extraction based on the effective Hamiltonian theory should be employed to accurately describe the physics of this regime. This is another complete story that will be the subject of a forthcoming paper.

Dedicacy : The authors wish to dedicate this article to Nadia Ben Amor, for her courage and tenacity in continuing to develop and maintain alone the CASDIloc program, without which an important part of our work based on wave functions analyses in orthogonal local orbitals would not have emerged.

Data availability statement : data available on request from the authors.

Bibliography

(1) Dzyaloshinsky, I. E. A Thermodynamic Theory of "Weak" Ferromagnetism of Antiferromagnetics. *J. Phys. Chem. Solids* **1958**, *4* (4), 241–255. https://doi.org/10.1016/0022-3697(58)90076-3.
(2) Moriya, T. Anisotropic Superexchange Interaction and Weak Ferromagnetism. *Phys. Rev.* **1960**, *120* (1), 91–98. https://doi.org/10.1103/PhysRev.120.91.
(3) Dzyaloshinskii, I. E. Theory of Helicoidal Structures in Antiferromagnets. I. Nonmetals. *JETP* **1963**, *19* (4), 960.
(4) Ishikawa, Y.; Tajima, K.; Bloch, D.; Roth, M. Helical Spin Structure in Manganese Silicide MnSi. *Solid State Commun.* **1976**, *19* (6), 525–528. https://doi.org/10.1016/0038-1098(76)90057-0.
(5) Haraldson, S.; Björn, L.; Beckman, O.; Smith, U. Magnetic Resonance in Cubic FeGe. *J. Magn. Reson. 1969* **1972**, *8* (3), 271–273. https://doi.org/10.1016/0022-2364(72)90009-1.
(6) Bak, P.; Jensen, M. H. Theory of Helical Magnetic Structures and Phase Transitions in MnSi and FeGe. *J. Phys. C Solid State Phys.* **1980**, *13* (31), L881. https://doi.org/10.1088/0022-3719/13/31/002.
(7) Kataoka, M.; Nakanishi, O. Helical Spin Density Wave Due to Antisymmetric Exchange Interaction. *J. Phys. Soc. Jpn.* **1981**, *50* (12), 3888–3896. https://doi.org/10.1143/JPSJ.50.3888.
(8) Bogdanov, A. N.; Yablonskii, D. A. Thermodynamically Stable "Vortices" in Magnetically Ordered Crystals. The Mixed State of Magnets. *JETP* **1989**, *68* (1), 101.
(9) Mandru, A.-O.; Yıldırım, O.; Tomasello, R.; Heistracher, P.; Penedo, M.; Giordano, A.; Suess, D.; Finocchio, G.; Hug, H. J. Coexistence of Distinct Skyrmion Phases Observed in Hybrid Ferromagnetic/Ferrimagnetic Multilayers. *Nat. Commun.* **2020**, *11* (1), 6365. https://doi.org/10.1038/s41467-020-20025-2.
(10) Yu, X. Z.; Onose, Y.; Kanazawa, N.; Park, J. H.; Han, J. H.; Matsui, Y.; Nagaosa, N.; Tokura, Y. Real-Space Observation of a Two-Dimensional Skyrmion Crystal. *Nature* **2010**, *465* (7300), 901–904. https://doi.org/10.1038/nature09124.
(11) Chen, G.; Mascaraque, A.; Jia, H.; Zimmermann, B.; Robertson, M.; Conte, R. L.; Hoffmann, M.; Barrio, M. A. G.; Ding, H.; Wiesendanger, R.; Michel, E. G.; Blügel, S.; Schmid, A. K.; Liu, K. Large Dzyaloshinskii-Moriya Interaction Induced by Chemisorbed Oxygen on a Ferromagnet Surface. *Sci. Adv.* **2020**, *6* (33), eaba4924. https://doi.org/10.1126/sciadv.aba4924.
(12) Khomskii, D. Classifying Multiferroics: Mechanisms and Effects. *Physics* **2009**, *2*, 20. https://doi.org/10.1103/Physics.2.20.
(13) Lottermoser, T.; Meier, D. A Short History of Multiferroics. *Phys. Sci. Rev.* **2020**, *1* (ahead-of-print). https://doi.org/10.1515/psr-2020-0032.
(14) Devonshire, A. F. Theory of Ferroelectrics. *Adv. Phys.* **1954**, *3* (10), 85–130. https://doi.org/10.1080/00018735400101173.
(15) Scott, J. F. Applications of Modern Ferroelectrics. *Science* **2007**, *315* (5814), 954–959. https://doi.org/10.1126/science.1129564.
(16) Yang, J. H.; Li, Z. L.; Lu, X. Z.; Whangbo, M.-H.; Wei, S.-H.; Gong, X. G.; Xiang, H. J. Strong Dzyaloshinskii-Moriya Interaction and Origin of Ferroelectricity in ${\mathrm{Cu}}_{2}{\mathrm{OSeO}}_{3}$. *Phys. Rev. Lett.* **2012**, *109* (10), 107203. https://doi.org/10.1103/PhysRevLett.109.107203.
(17) Schmid, H. Multi-Ferroic Magnetoelectrics. *Ferroelectrics* **1994**, *162* (1), 317–338. https://doi.org/10.1080/00150199408245120.
(18) Buckingham, A. D.; Pyykkö, P.; Robert, J. B.; Wiesenfeld, L. Symmetry Rules for the Indirect Nuclear Spin-Spin Coupling Tensor Revisited. *Mol. Phys.* **1982**, *46* (1), 177–182. https://doi.org/10.1080/00268978200101171.
(19) Chibotaru, L. F.; Ungur, L.; Aronica, C.; Elmoll, H.; Pilet, G.; Luneau, D. Structure, Magnetism, and Theoretical Study of a Mixed-Valence $Co^{II}_3 Co^{III}_4$ Heptanuclear Wheel:

Lack of SMM Behavior despite Negative Magnetic Anisotropy. *J. Am. Chem. Soc.* **2008**, *130* (37), 12445–12455. https://doi.org/10.1021/ja8029416.

(20) Soncini, A.; Chibotaru, L. F. Toroidal Magnetic States in Molecular Wheels: Interplay between Isotropic Exchange Interactions and Local Magnetic Anisotropy. *Phys. Rev. B* **2008**, *77* (22), 220406. https://doi.org/10.1103/PhysRevB.77.220406.

(21) Neese, F. Calculation of the Zero-Field Splitting Tensor on the Basis of Hybrid Density Functional and Hartree-Fock Theory. *J. Chem. Phys.* **2007**, *127* (16), 164112. https://doi.org/10.1063/1.2772857.

(22) Ganyushin, D.; Neese, F. First-Principles Calculations of Zero-Field Splitting Parameters. *J. Chem. Phys.* **2006**, *125* (2), 024103. https://doi.org/10.1063/1.2213976.

(23) Sayfutyarova, E. R.; Chan, G. K.-L. A State Interaction Spin-Orbit Coupling Density Matrix Renormalization Group Method. *J. Chem. Phys.* **2016**, *144* (23), 234301. https://doi.org/10.1063/1.4953445.

(24) Ruiz, E.; Cirera, J.; Cano, J.; Alvarez, S.; Loose, C.; Kortus, J. Can Large Magnetic Anisotropy and High Spin Really Coexist? *Chem. Commun.* **2007**, No. 1, 52–54. https://doi.org/10.1039/B714715E.

(25) Maurice, R.; Guihéry, N.; Bastardis, R.; Graaf, C. de. Rigorous Extraction of the Anisotropic Multispin Hamiltonian in Bimetallic Complexes from the Exact Electronic Hamiltonian. *J. Chem. Theory Comput.* **2010**, *6* (1), 55–65. https://doi.org/10.1021/ct900473u.

(26) Maurice, R.; Bastardis, R.; Graaf, C. de; Suaud, N.; Mallah, T.; Guihéry, N. Universal Theoretical Approach to Extract Anisotropic Spin Hamiltonians. *J. Chem. Theory Comput.* **2009**, *5* (11), 2977–2984. https://doi.org/10.1021/ct900326e.

(27) Liu, W. *Handbook of Relativistic Quantum Chemistry*; Springer Berlin Heidelberg: New York, NY, 2016.

(28) Maurice, R.; Sivalingam, K.; Ganyushin, D.; Guihéry, N.; de Graaf, C.; Neese, F. Theoretical Determination of the Zero-Field Splitting in Copper Acetate Monohydrate. *Inorg. Chem.* **2011**, *50* (13), 6229–6236. https://doi.org/10.1021/ic200506q.

(29) Maurice, R.; de Graaf, C.; Guihéry, N. Magnetic Anisotropy in Binuclear Complexes in the Weak-Exchange Limit: From the Multispin to the Giant-Spin Hamiltonian. *Phys. Rev. B* **2010**, *81* (21), 214427. https://doi.org/10.1103/PhysRevB.81.214427.

(30) Ruamps, R.; Maurice, R.; de Graaf, C.; Guihéry, N. Interplay between Local Anisotropies in Binuclear Complexes. *Inorg. Chem.* **2014**, *53* (9), 4508–4516. https://doi.org/10.1021/ic500180k.

(31) Maurice, R.; Pradipto, A. M.; Guihéry, N.; Broer, R.; de Graaf, C. Antisymmetric Magnetic Interactions in Oxo-Bridged Copper(II) Bimetallic Systems. *J. Chem. Theory Comput.* **2010**, *6* (10), 3092–3101. https://doi.org/10.1021/ct100329n.

(32) Pradipto, A.-M.; Maurice, R.; Guihéry, N.; de Graaf, C.; Broer, R. First-Principles Study of Magnetic Interactions in Cupric Oxide. *Phys. Rev. B* **2012**, *85* (1). https://doi.org/10.1103/PhysRevB.85.014409.

(33) Maurice, R.; Pradipto, A.-M.; de Graaf, C.; Broer, R. Magnetic Interactions in LiCu2O2: Single-Chain versus Double-Chain Models. *Phys. Rev. B* **2012**, *86* (2), 024411. https://doi.org/10.1103/PhysRevB.86.024411.

(34) Bogdanov, N. A.; Maurice, R.; Rousochatzakis, I.; van den Brink, J.; Hozoi, L. Magnetic State of Pyrochlore Cd 2 Os 2 O 7 Emerging from Strong Competition of Ligand Distortions and Longer-Range Crystalline Anisotropy. *Phys. Rev. Lett.* **2013**, *110* (12), 127206. https://doi.org/10.1103/PhysRevLett.110.127206.

(35) Atanasov, M.; Comba, P.; Hanson, G. R.; Hausberg, S.; Helmle, S.; Wadepohl, H. Cyano-Bridged Homodinuclear Copper(II) Complexes. *Inorg. Chem.* **2011**, *50* (15), 6890–6901. https://doi.org/10.1021/ic102430a.

(36) Moskvin, A. S. Dzyaloshinsky-Moriya Antisymmetric Exchange Coupling in Cuprates: Oxygen Effects. *J. Exp. Theor. Phys.* **2007**, *104* (6), 913–927. https://doi.org/10.1134/S106377610706009X.

(37) Kauffmann, K. E.; Popescu, C. V.; Dong, Y.; Lipscomb, J. D.; Que, Lawrence; Münck, E. Mössbauer Evidence for Antisymmetric Exchange in a Diferric Synthetic Complex and Diferric Methane Monooxygenase. *J. Am. Chem. Soc.* **1998**, *120* (34), 8739–8746. https://doi.org/10.1021/ja981065t.

(38) Yoon, J.; Mirica, L. M.; Stack, T. D. P.; Solomon, E. I. Spectroscopic Demonstration of a Large Antisymmetric Exchange Contribution to the Spin-Frustrated Ground State of a D3 Symmetric Hydroxy-Bridged Trinuclear Cu(II) Complex: Ground-to-Excited State Superexchange Pathways. *J. Am. Chem. Soc.* **2004**, *126* (39), 12586–12595. https://doi.org/10.1021/ja046380w.

(39) Aquilante, F.; De Vico, L.; Ferré, N.; Ghigo, G.; Malmqvist, P. Å.; Neogrády, P.; Pedersen, T. B.; Pitoňák, M.; Reiher, M.; Roos, B. O.; Serrano-Andrés, L.; Urban, M.; Veryazov, V.; Lindh, R. MOLCAS 7: The Next Generation. *J. Comput. Chem.* **2010**, *31* (1), 224–247. https://doi.org/10.1002/jcc.21318.

(40) Karlström, G.; Lindh, R.; Malmqvist, P.-Å.; Roos, B. O.; Ryde, U.; Veryazov, V.; Widmark, P.-O.; Cossi, M.; Schimmelpfennig, B.; Neogrady, P.; Seijo, L. MOLCAS: A Program Package for Computational Chemistry. *Comput. Mater. Sci.* **2003**, *28* (2), 222–239. https://doi.org/10.1016/S0927-0256(03)00109-5.

(41) Aquilante, F.; Autschbach, J.; Carlson, R. K.; Chibotaru, L. F.; Delcey, M. G.; De Vico, L.; Fdez. Galván, I.; Ferré, N.; Frutos, L. M.; Gagliardi, L.; Garavelli, M.; Giussani, A.; Hoyer, C. E.; Li Manni, G.; Lischka, H.; Ma, D.; Malmqvist, P. Å.; Müller, T.; Nenov, A.; Olivucci, M.; Pedersen, T. B.; Peng, D.; Plasser, F.; Pritchard, B.; Reiher, M.; Rivalta, I.; Schapiro, I.; Segarra-Martí, J.; Stenrup, M.; Truhlar, D. G.; Ungur, L.; Valentini, A.; Vancoillie, S.; Veryazov, V.; Vysotskiy, V. P.; Weingart, O.; Zapata, F.; Lindh, R. Molcas 8: New Capabilities for Multiconfigurational Quantum Chemical Calculations across the Periodic Table: Molcas 8. *J. Comput. Chem.* **2016**, *37* (5), 506–541. https://doi.org/10.1002/jcc.24221.

(42) Malmqvist, P. Å.; Rendell, A.; Roos, B. O. The Restricted Active Space Self-Consistent-Field Method, Implemented with a Split Graph Unitary Group Approach. *J. Phys. Chem.* **1990**, *94* (14), 5477–5482. https://doi.org/10.1021/j100377a011.

(43) Maynau, D.; Evangelisti, S.; Guihéry, N.; Calzado, C. J.; Malrieu, J.-P. Direct Generation of Local Orbitals for Multireference Treatment and Subsequent Uses for the Calculation of the Correlation Energy. *J. Chem. Phys.* **2002**, *116* (23), 10060–10068. https://doi.org/10.1063/1.1476312.

(44) Ben Amor, N.; Bessac, F.; Hoyau, S.; Maynau, D. Direct Selected Multireference Configuration Interaction Calculations for Large Systems Using Localized Orbitals. *J. Chem. Phys.* **2011**, *135*, 014101/1-014101/14. https://doi.org/10.1063/1.3600351.

(45) Malmqvist, P. Å.; Roos, B. O.; Schimmelpfennig, B. The Restricted Active Space (RAS) State Interaction Approach with Spin–Orbit Coupling. *Chem. Phys. Lett.* **2002**, *357* (3–4), 230–240. https://doi.org/10.1016/S0009-2614(02)00498-0.

(46) Aquilante, F.; Pedersen, T. B.; Sánchez de Merás, A.; Koch, H. Fast Noniterative Orbital Localization for Large Molecules. *J. Chem. Phys.* **2006**, *125* (17), 174101. https://doi.org/10.1063/1.2360264.

(47) Dunn, T. M. Spin-Orbit Coupling in the First and Second Transition Series. *Trans. Faraday Soc.* **1961**, *57* (0), 1441–1444. https://doi.org/10.1039/TF9615701441.

(48) Ruamps, R.; Maurice, R.; Batchelor, L.; Boggio-Pasqua, M.; Guillot, R.; Barra, A. L.; Liu, J.; Bendeif, E.-E.; Pillet, S.; Hill, S.; Mallah, T.; Guihéry, N. Giant Ising-Type Magnetic Anisotropy in Trigonal Bipyramidal Ni(II) Complexes: Experiment and Theory. *J. Am. Chem. Soc.* **2013**, *135* (8), 3017–3026. https://doi.org/10.1021/ja308146e.

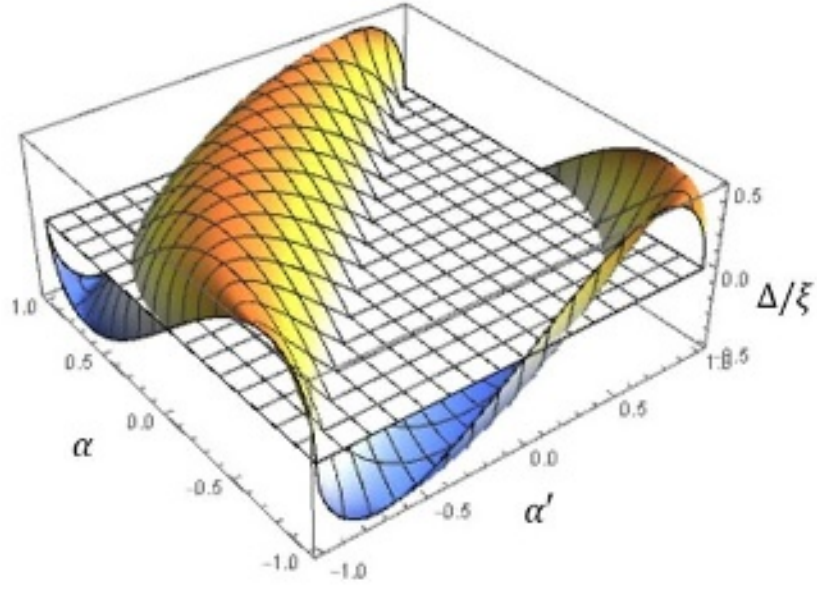
1.0
0.5
0.0
−0.5
−1.0
α
α′
Δ/ξ

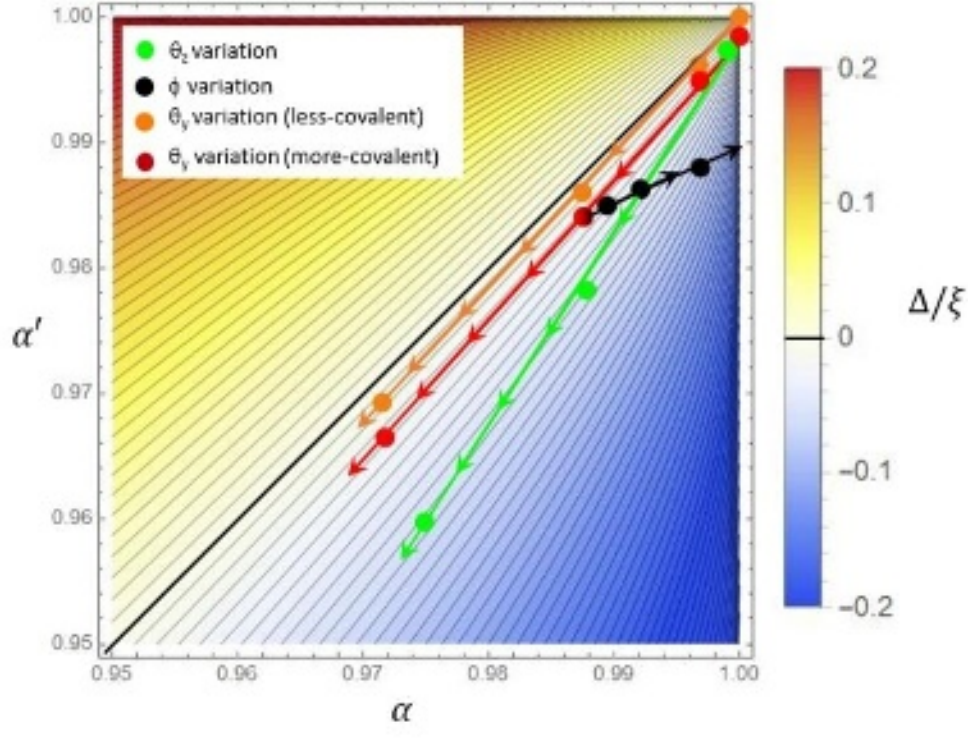
θz variation
ϕ variation
θy variation (less-covalent)
θy variation (more-covalent)
α′
α
Δ/ξ

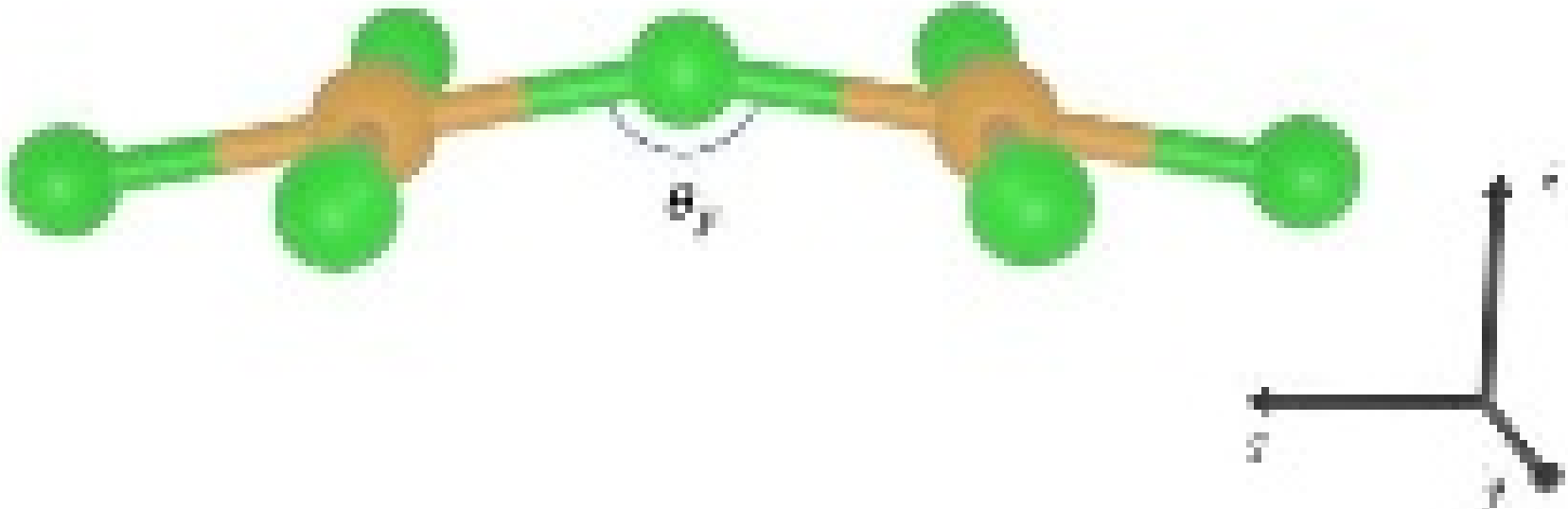
θ_y
z
x
y

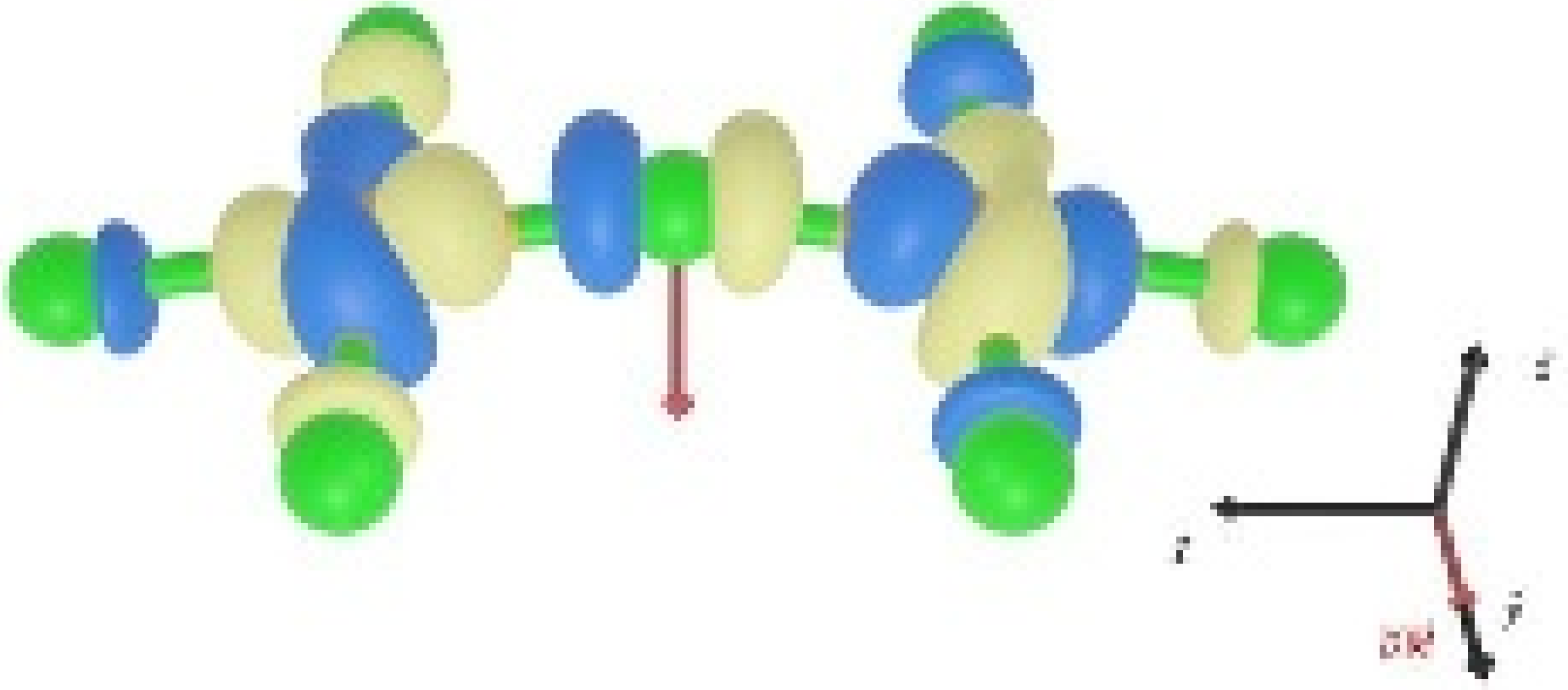
z
x
y
CN

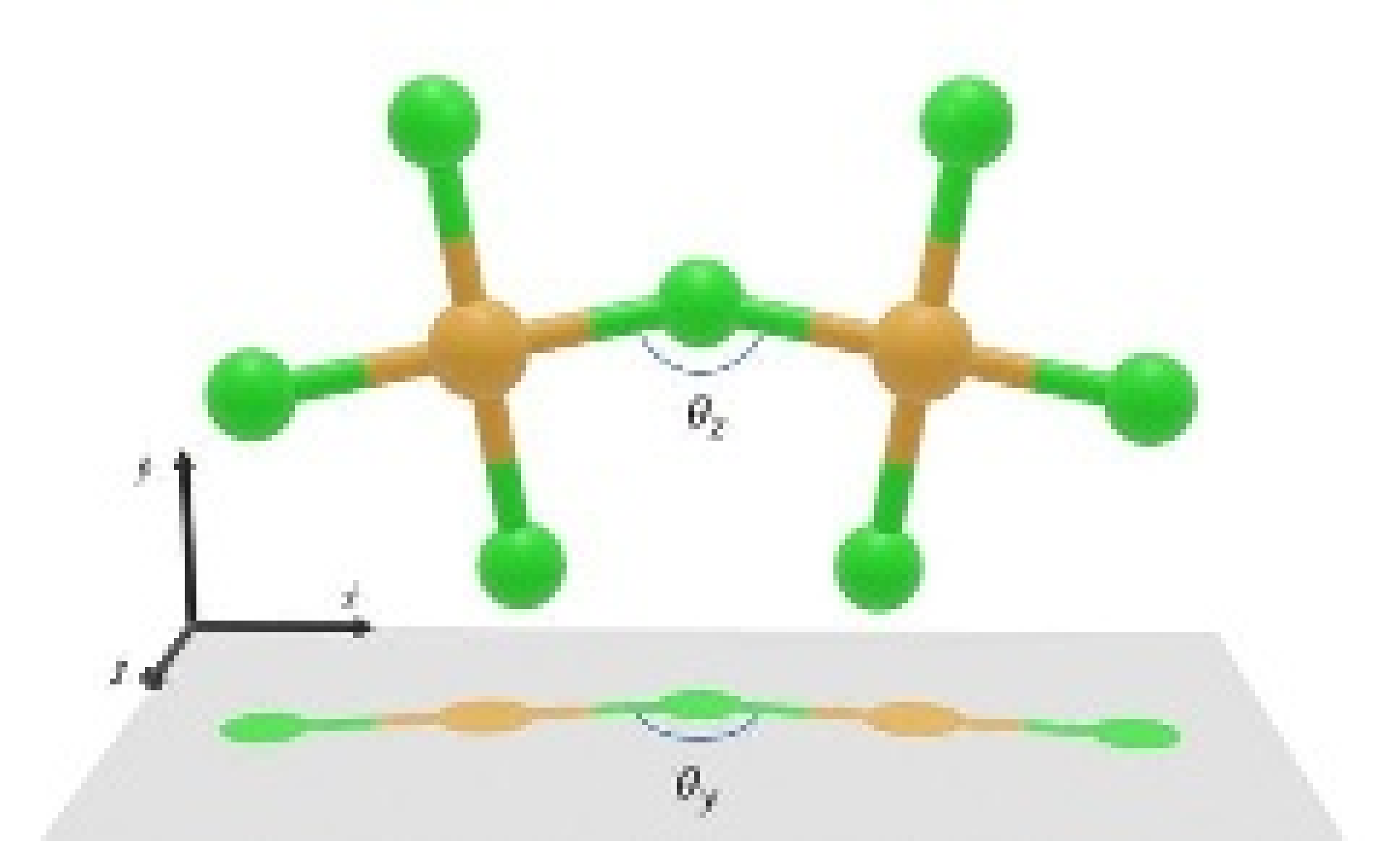
θ_z
θ_y
z
x
y

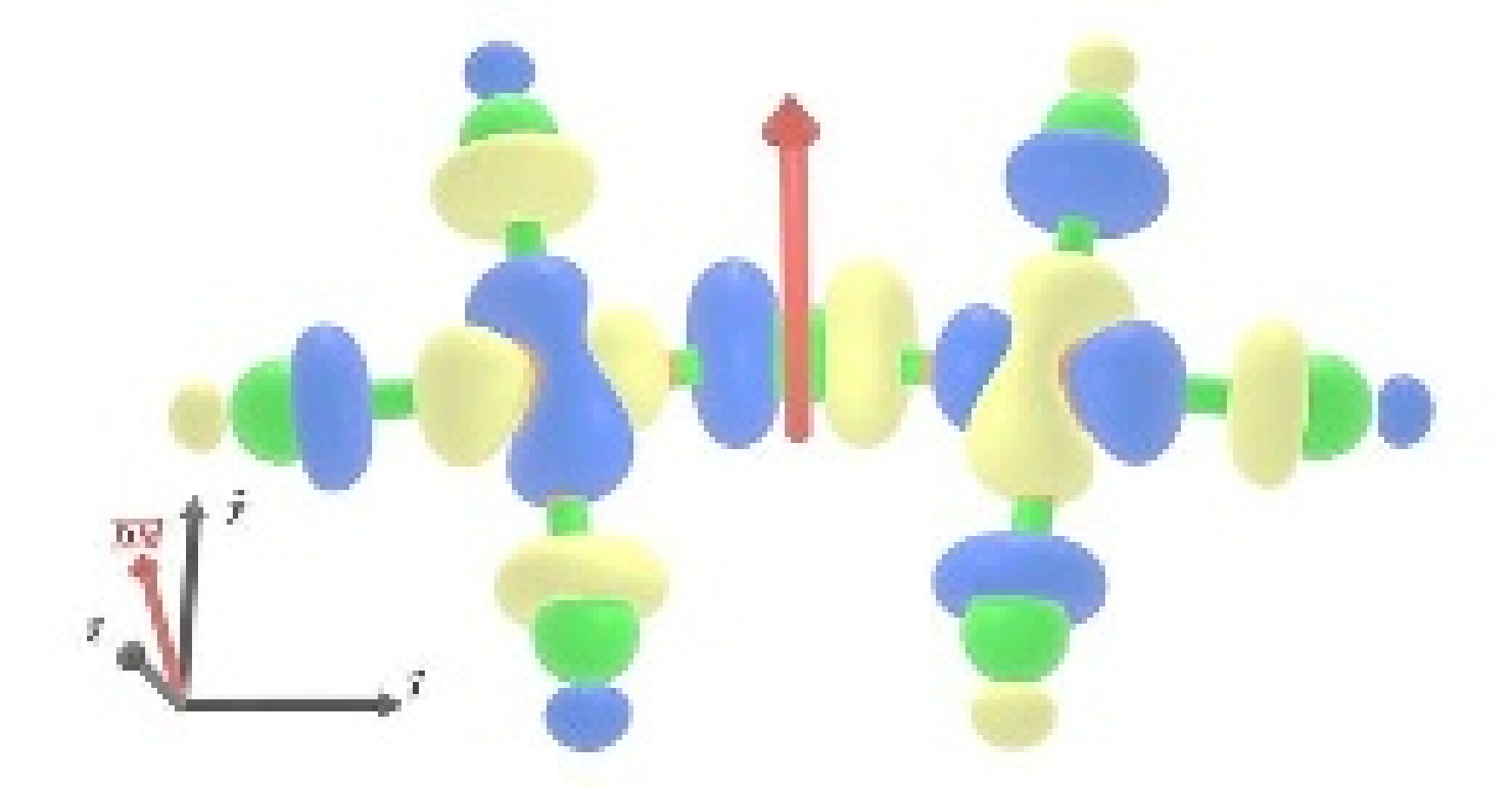
z
x
y

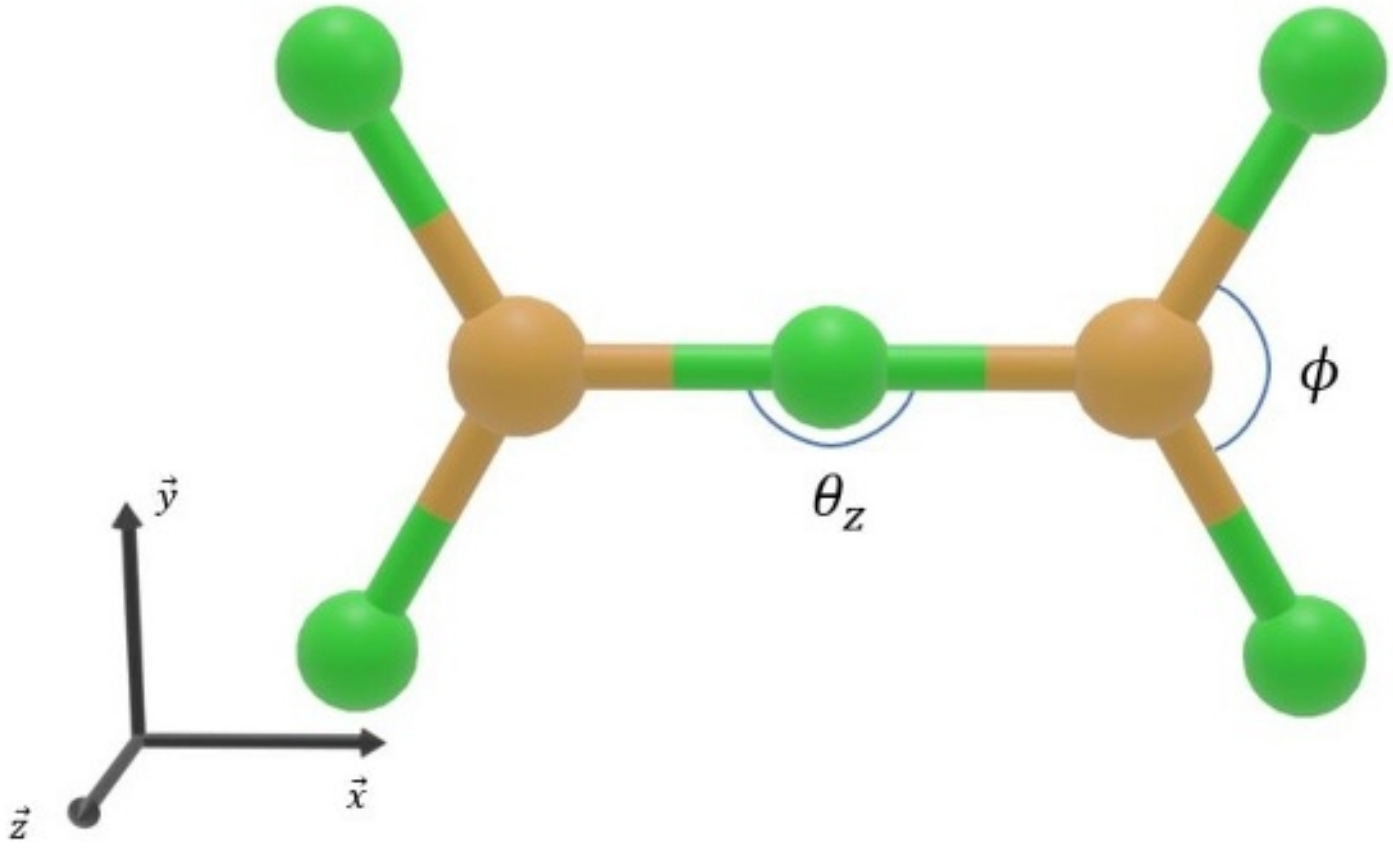
$\vec{y}$
$\vec{x}$
$\vec{z}$
θ_z
ϕ

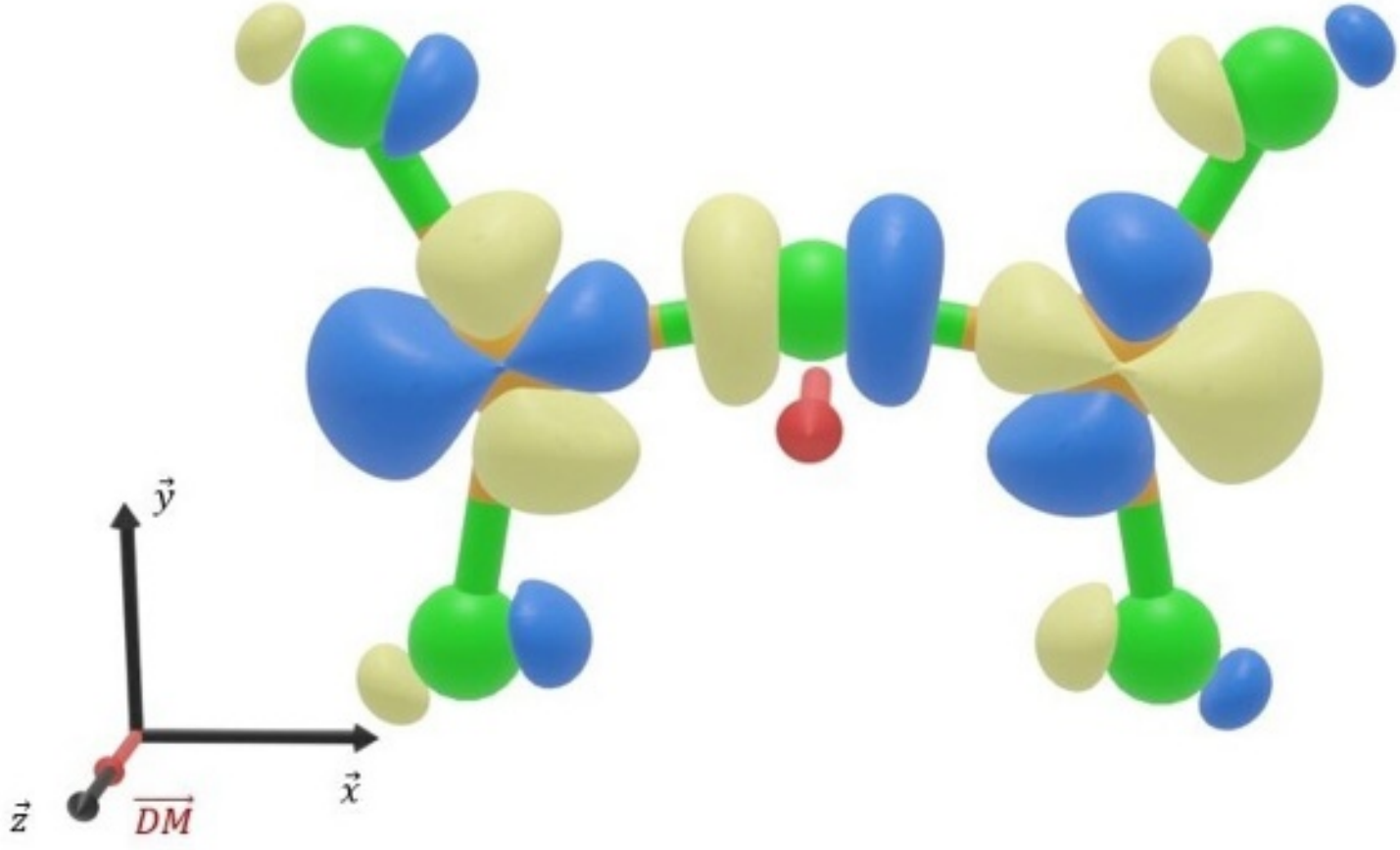
$\vec{y}$
$\vec{x}$
$\vec{z}$
$\overrightarrow{DM}$

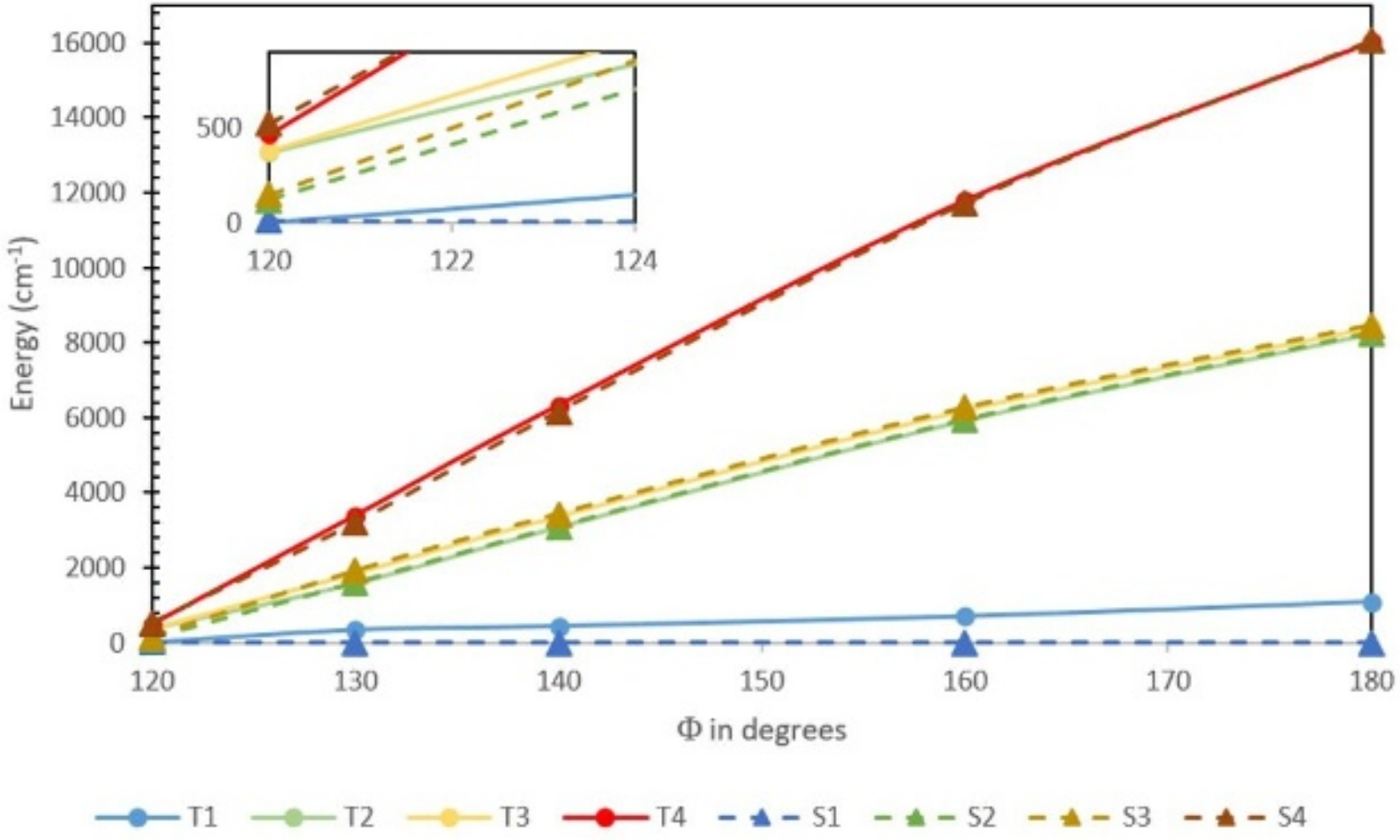
16000
14000
12000
10000
8000
6000
4000
2000
0
Energy (cm-1)
500
0
120
122
124
120
130
140
150
160
170
180
Φ in degrees
T1
T2
T3
T4
S1
S2
S3
S4